





Organoselenium Has a Potent Fungicidal Effect on *Cryptococcus neoformans* and Inhibits the Virulence Factors

Daniel Felipe Freitas De Jesus,^a Aline Luiza Duarte De Freitas,^a Isadora Maria De Oliveira,^b Larissa Costa De Almeida,^a Rafael Wesley Bastos,^c Cristina de Castro Spadari,^a Analy Sales de Azevedo Melo,^d Daniel de Assis Santos,^e  Leticia Veras Costa-Lotufo,^a Flavia C. G. Reis,^{f,g} Marcio L. Rodrigues,^{f,h} Hélio Alexandre Stefani,^b  Kelly Ishida^a

^aInstitute of Biomedical Sciences, University of São Paulo (USP), São Paulo, Brazil

^bSchool of Pharmaceutical Sciences, University of São Paulo (USP), São Paulo, Brazil

^cCenter of Biosciences, Federal University of Rio Grande do Norte (UFRN), Natal, Brazil

^dDepartment of Medicine, Federal University of São Paulo (UNIFESP), São Paulo, Brazil

^eInstitute of Biomedical Sciences, Federal University of Minas Gerais (UFMG), Belo Horizonte, Brazil

^fCarlos Chagas Institute, Oswaldo Cruz Foundation, Curitiba, Brazil

^gCenter for Technological Development in Health (CDTS), Oswaldo Cruz Foundation, Rio de Janeiro, Brazil

^hInstitute of Microbiology Paulo de Góes, Federal University of Rio de Janeiro (UFRJ), Rio de Janeiro, Brazil

ABSTRACT Cryptococcosis therapy is often limited by toxicity problems, antifungal tolerance, and high costs. Studies approaching chalcogen compounds, especially those containing selenium, have shown promising antifungal activity against pathogenic species. This work aimed to evaluate the *in vitro* and *in vivo* antifungal potential of organoselenium compounds against *Cryptococcus neoformans*. The lead compound LQA_78 had an inhibitory effect on *C. neoformans* planktonic cells and dispersed cells from mature biofilms at similar concentrations. The fungal growth inhibition led to an increase in budding cells arrested in the G₂/M phase, but the compound did not significantly affect structural cell wall components or chitinase activity, an enzyme that regulates the dynamics of the cell wall. The compound also inhibited titan cell (Tc) and enlarged capsule yeast (NcC) growth and reduced the body diameter and capsule thickness associated with increased capsular permeability of both virulent morphotypes. LQA_78 also reduced fungal melanization through laccase activity inhibition. The fungicidal activity was observed at higher concentrations (16 to 64 μg/mL) and may be associated with augmented plasma membrane permeability, ROS production, and loss of mitochondrial membrane potential. While LQA_78 is a nonhemolytic compound, its cytotoxic effects were cell type dependent, exhibiting no toxicity on *Galleria mellonella* larvae at a dose ≤46.5 mg/kg. LQA_78 treatment of larvae infected with *C. neoformans* effectively reduced the fungal burden and inhibited virulent morphotype formation. To conclude, LQA_78 displays fungicidal action and inhibits virulence factors of *C. neoformans*. Our results highlight the potential use of LQA_78 as a lead molecule for developing novel pharmaceuticals for treating cryptococcosis.

KEYWORDS *Cryptococcus*, titan cell, capsule, antifungal, selenium, quinoline, *Galleria mellonella*, virulence

The fungus *Cryptococcus neoformans* is a known etiological agent of cryptococcal meningitis (CM), the severe form of cryptococcosis (1). The fungi often infect immunocompromised individuals (e.g., HIV/AIDS patients) vulnerable to cerebral dissemination by the yeasts (2). It was previously estimated that 278,000 cases of cryptococcosis occur annually, with 223,100 cases progressing to CM, which is associated with a high (181,100 deaths) mortality rate (1), thus, becoming an emerging public health problem in several countries (3).

The pathogenesis of CM has been associated with several fungal virulence factors. For example, components of the cell wall and polysaccharide capsule, melanin and

Copyright © 2023 American Society for Microbiology. All Rights Reserved.

Address correspondence to Kelly Ishida, ishidakelly@usp.br.

The authors declare no conflict of interest.

Received 30 May 2022

Returned for modification 3 July 2022

Accepted 14 January 2023

Published 23 February 2023

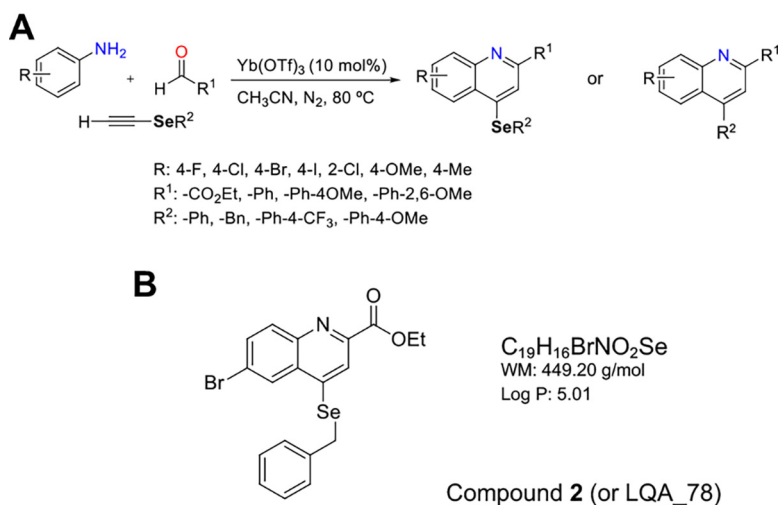


FIG 1 Quinoline compounds. (A) Summary route of synthesis of quinoline compounds containing or not the selenium atom (1–27). (B) Chemical structure of compound 2.

enzyme production, the ability to adhere and form biofilms, and the morphogenesis of regular (normal) cells into microcells and titan cells (Tc) contribute to brain infection and fungal dissemination (4, 5).

Currently, anticryptococcal therapy is limited to three antifungal classes: polyenes (amphotericin B and its lipid formulations), azoles (fluconazole), and pyrimidine analogs (5-flucytosine) (6). In addition to the limited number of antifungals available, the fungi's genomic and physiological plasticity, which leads to the emergence of resistance to traditional antifungals, is a great challenge in treating cryptococcosis (7). Consequently, these two obstacles have hampered therapeutic options and contributed to treatment failure (8). Therefore, there is an urgent need for pharmacological alternatives for treating cryptococcosis.

Recently, compounds with a quinoline core were shown to exhibit antifungal activity (9), and selenium-based compounds were effective against different fungal pathogenic species (10). However, the utility of these molecules as antifungals has been little explored. The present study evaluated organoselenium compounds containing a quinoline core as potential antifungals, seeking to identify leader molecules that could lead to new strategies for treating *Cryptococcus*-infected patients.

RESULTS

Screening for antifungal activity and selection of the lead molecule. Twenty-seven compounds were screened for antifungal activity against three representative fungal species of clinical importance (*C. neoformans*, *C. albicans*, and *A. fumigatus*) (Fig. 1A and Table S1). Only 11 compounds inhibited *C. neoformans* and/or *C. albicans* with MIC of 50% (IC₅₀) values $\leq 64 \mu\text{g/mL}$. While *C. neoformans* was more susceptible than *C. albicans*, none of the compounds had an inhibitory effect on *A. fumigatus* (Table S1). Among them, compound 2 (here named LQA_78, Fig. 1B) displayed the greatest antifungal potential, inhibiting *C. neoformans* (ICs = 4 to 8 $\mu\text{g/mL}$) and *C. albicans* (ICs = 8 to 16 $\mu\text{g/mL}$) with a substantial fungicidal effect against both species (Table S1). In addition, none of the tested compounds caused hemolysis, not even in the highest tested concentration (128 $\mu\text{g/mL}$) (Table S1).

Due to its low inhibitory concentrations, observed fungicidal action, and lack of hemolytic activity, compound LQA_78 was selected for subsequent *in vitro* and *in vivo* trials against *C. neoformans* strains.

LQA_78 has inhibitory and fungicidal effects against *Cryptococcus neoformans*, and its cytotoxicity is cell lineage dependent. Amphotericin B (AMB) was the most effective antifungal against *C. neoformans* strains ($n = 17$), exhibiting the lowest IC values and fungicidal action, while fluconazole (FLC) inhibited the fungal growth at 0.25 to 8 $\mu\text{g/mL}$

TABLE 1 Susceptibility of *Cryptococcus neoformans* strains to the organoselenium compound LQA_78 and the standard antifungals fluconazole and amphotericin B^a

| Compounds | Concentrations ($\mu\text{g/mL}$) | | |
|----------------|-------------------------------------|------------------|--------|
| | IC ₅₀ | IC ₉₀ | MFC |
| Amphotericin B | | | |
| Median | 0.06 | 0.25 | 0.375 |
| Range | 0.016–0.25 | 0.03–0.5 | 0.03–1 |
| Fluconazole | | | |
| Median | 2 | 4 | 8 |
| Range | 0.25–4 | 0.25–8 | 2–64 |
| LQA_78 | | | |
| Median | 8 | 16 | 32 |
| Range | 1–16 | 2–32 | 4–64 |

^aIC₅₀: lowest concentration that inhibits 50% of fungal growth; IC₉₀: lowest concentration that inhibits 90% of fungal growth; MFC: lowest concentration that kills >99.9% of yeasts. The assays were performed in duplicate at least three times. The data represent the modal mean.

(Table 1 and Table S2). According to the previously reported epidemiological cutoff values (11), none of the *C. neoformans* clinical isolates were resistant to AMB or FLC.

Compound LQA_78 had an inhibitory effect at 1 to 32 $\mu\text{g/mL}$ and fungicidal effect at 4 to 64 $\mu\text{g/mL}$ against all *C. neoformans* strains, including the H99 adapted (A) strain, which displayed higher FLC IC values compared to its counterpart H99 nonadapted (NA) strain (Table 1 and Table S2). The combinations of LQA_78 with FLC or AMB revealed indifferent interactions (FICI >0.5 and <4.0).

LQA_78 was also tested against four cell lineages. Its cytotoxicity effect was cell type dependent, with a lower cytotoxic concentration of 50% (CC₅₀) in fibroblasts, intermediary cytotoxicity on colorectal carcinoma cells and macrophages, and noncytotoxic effect on breast adenocarcinoma cells (MCF-7), and consequent variable selectivity index (SI from 4.93 to >12.50) (Table 2).

LQA_78 inhibits the fungal growth, arresting yeasts in the G₂/M phase. *C. neoformans* (H99[NA], H99[A], and L354 strains) treated with LQA_78 had a significant increase (30 to 50%) in budding yeasts compared to untreated yeasts (Fig. 2A–C and Fig. S1). Additionally, LQA_78 induced a significant increase in the yeast population in the G₂/M phase of the cell cycle, consequently impairing cell separation (Fig. 2D).

The chitinase activity of *C. neoformans* was also evaluated. No difference was observed between untreated and treated yeast cells. Accordingly, both manifested a similar pattern of chitooligomer distribution (Fig. 2B, C, and E). Since chitooligomers are the products of the enzymatic hydrolysis of chitin during bud separation, these results are consistent with a similar detection of chitinase in untreated and drug-treated cells.

LQA_78 inhibits dispersed cells from mature *Cryptococcus neoformans* biofilms. LQA_78 inhibited the growth of dispersed cells from *C. neoformans* biofilms at similar concentrations for planktonic cells (Table 3 and Table S2). However, it did not inhibit the sessile cells from mature biofilms even at the highest tested concentration. In con-

TABLE 2 Half maximal cytotoxic concentration (CC₅₀) and 95% confidence interval (CI95%) of LQA_78 on nontumoral fibroblasts (CCD18Co), colorectal carcinoma (HCT116), breast adenocarcinoma (MCF-7), and macrophages (J774A.1)^a

| Cell lineages | Concentrations ($\mu\text{g/mL}$) | | Selectivity index (SI) ^b |
|---------------|-------------------------------------|--------------|-------------------------------------|
| | CC ₅₀ | CI 95% | |
| CCD-18Co | 2.97 | 1.54–5.76 | ND |
| HCT116 | 39.48 | 15.24–159.29 | 4.93 |
| MCF7 | >100 | ND | >12.50 |
| J774A.1 | 15.81 | 12.23–20.44 | 1.97 |

^aND, not determined.

^bCC₅₀/IC₅₀ median. The assays were performed, in triplicate, at least twice.

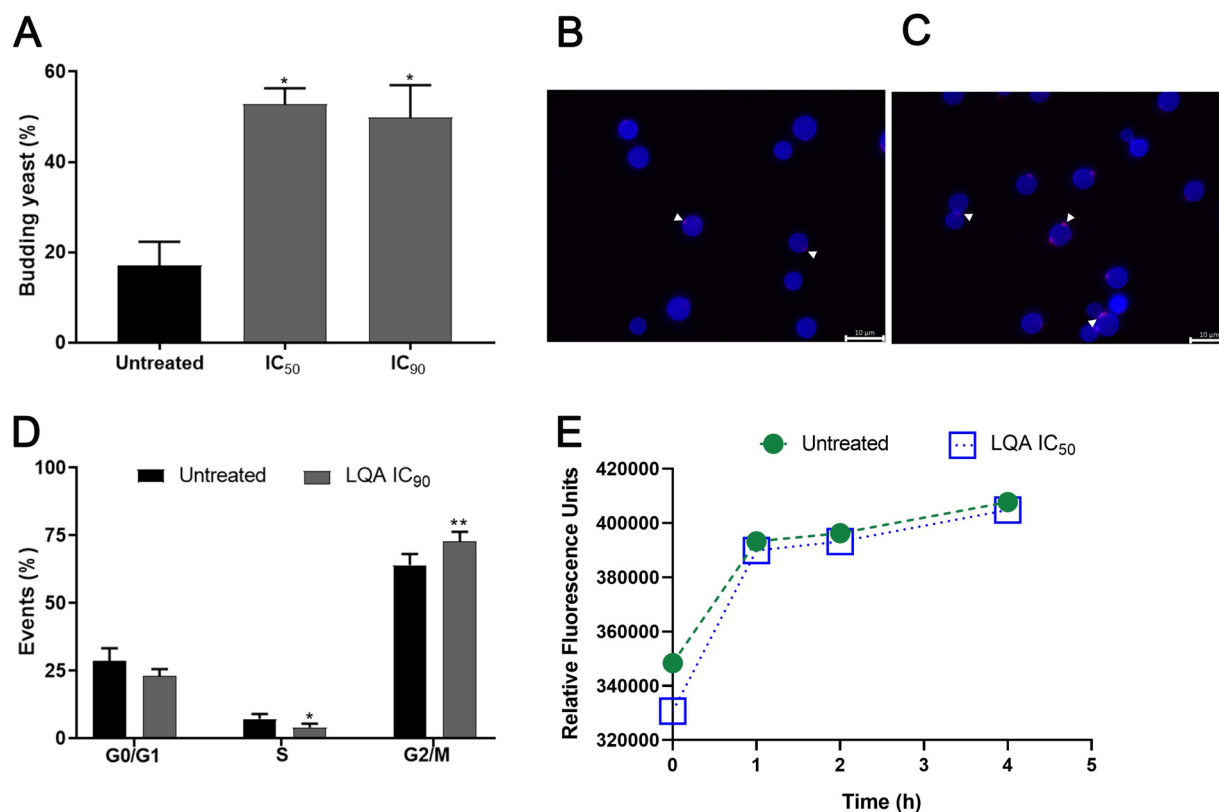


FIG 2 LQA_78 affects *Cryptococcus neoformans* H99 cell cycle. (A) Budding percentage in the yeasts treated with 4 μg/mL (IC₅₀) and 8 μg/mL (IC₉₀). (B) Untreated and (C) treated yeasts observed by fluorescence microscopy highlighting budding-yeast and presence of chitin (blue color) and chitooligomers (pink color indicated by white arrowheads). (D) Cell cycle evaluation by propidium iodide labeling. (E) Chitinase activity. *, *P* < 0.05; and **, *P* < 0.01 compared with the untreated group of two independent experiments, in duplicate (A and E) and triplicate (D) (one-way ANOVA with Dunnett’s posttest).

trast, AMB had antibiofilm activity on both sessile and dispersed cells from mature *C. neoformans* biofilms (Table 3).

LQA_78 is active toward *Cryptococcus neoformans* morphotypes and affects the capsular permeability. The morphotypes of normal cells with enlarged capsule thickness (NcC) and titan cells (Tc) obtained from normal cells (Nc) of the H99(NA), H99(A), and L354 strains were susceptible to LQA_78 at concentrations close to those found for Nc (Table 4). Interestingly, this compound was active against morphotypes of the H99(A) strain that showed lower susceptibility to FLC (Table 4).

The LQA_78 treatment induced a significant decrease in cell body diameter and capsular thickness of NcC, Tc and Nc cells (Fig. 3A–I and Fig. S2A–D). The compound increased the capsular permeability in the NcC, resulting in 60 to 70% cell labeling with the fluorophore rhodamine isothiocyanate-dextran 70 kDa (Fig. 3J and K and Fig. S2E and F). On the

TABLE 3 Antibiofilm activity of amphotericin B (AMB) and compound LQA_78 on sessile and dispersed cells from mature biofilms of H99 nonadapted (NA), H99 adapted (A), and clinical isolate (L354) of *Cryptococcus neoformans*^a

| Strains | Sessile cells | | | | Dispersed cells | | | |
|---------|-------------------|-------------------|-------------------|-------------------|-------------------|-------------------|-------------------|-------------------|
| | AMB | | LQA_78 | | AMB | | LQA_78 | |
| | BIC ₅₀ | BIC ₉₀ | BIC ₅₀ | BIC ₉₀ | BIC ₅₀ | BIC ₉₀ | BIC ₅₀ | BIC ₉₀ |
| H99 NA | 0.06 | 0.25 | >128 | >128 | 0.016 | 0.016 | 8 | >128 |
| H99 A | 0.25 | 0.5 | >128 | >128 | 0.016 | 0.016 | 1 | >128 |
| L354 | 4 | 16 | >128 | >128 | 0.03 | 0.06 | 8 | 32 |

^aBICs: MICs that reduce the metabolic activity of sessile cells or inhibit the growth of dispersed cells by 50% (BIC₅₀) and 90% (BIC₉₀). The concentration values are depicted in μg/mL. The assays were performed in triplicate at least twice. The data represent the modal mean.

TABLE 4 Susceptibility of *Cryptococcus neoformans* morphotypes to organoselenium LQA_78 and standard antifungals fluconazole (FLC) and amphotericin B (AMB)^a

| Strains/morphotypes | AMB | | | FLC | | | LQA_78 | | |
|---------------------|------------------|------------------|------|------------------|------------------|-----|------------------|------------------|-----|
| | IC ₅₀ | IC ₉₀ | MFC | IC ₅₀ | IC ₉₀ | MFC | IC ₅₀ | IC ₉₀ | MFC |
| H99 NA | | | | | | | | | |
| Nc | 0.016 | 0.03 | 0.06 | 1 | 2 | 8 | 4 | 8 | 16 |
| NcC | 0.03 | 0.03 | 0.06 | 2 | 4 | 32 | 8 | 16 | 32 |
| Tc | 0.03 | 0.06 | 0.06 | 2 | 8 | 8 | 8 | 16 | 32 |
| H99 A | | | | | | | | | |
| Nc | 0.016 | 0.03 | 0.06 | 4 | 8 | 64 | 4 | 8 | 16 |
| NcC | 0.06 | 0.125 | 0.25 | 32 | 64 | >64 | 4 | 8 | 32 |
| Tc | 0.016 | 0.03 | 0.25 | 32 | 64 | >64 | 8 | 16 | 32 |
| L354 | | | | | | | | | |
| Nc | 0.25 | 0.25 | 0.5 | 4 | 8 | 16 | 8 | 16 | 32 |
| NcC | 0.03 | 0.125 | 0.5 | 4 | 8 | 16 | 4 | 8 | 16 |
| Tc | 0.25 | 0.5 | 0.5 | 4 | 8 | 16 | 4 | 8 | 16 |

^aIC₅₀: lowest concentration that inhibits 50% of fungal growth; IC₉₀: lowest concentration that inhibits 90% of fungal growth; MFC: lowest concentration that kills >99.9% of yeasts. Nc, normal cells; NcC, enlarged capsule yeasts; Tc, titan cells. The concentration values are expressed in $\mu\text{g}/\text{mL}$. The assays were performed in duplicate at least three times. The data represent the modal mean.

other hand, encapsulated and untreated cells were less intensely stained because the dye had difficulties crossing the capsule (12).

Effect of LQA_78 on melanization and laccase activity. LQA_78 at inhibitory concentrations inhibited colony melanization of *C. neoformans* strains (Fig. 4A, D, and G). Furthermore, no difference in the melanin amount was detected in the supernatant of the untreated and treated yeasts using liquid medium (Fig. S3A–C).

Laccase activity was observed in both supernatant and yeasts of untreated *C. neoformans* strains (H99[NA], H99[A], and L354). LQA_78 inhibited the laccase activity by more than 50% in the supernatant and yeasts at different incubation times (Fig. 4). We observed an inhibitory effect of LQA_78 on the laccase activity of the H99(NA) (Fig. 4B and C) and H99(A) (Fig. 4E and F) strains. This compound most prominently inhibited the L354 strain's laccase activity at both concentrations (IC₅₀ and IC₉₀), which remained inhibited for up to 24 h of incubation in the supernatant and yeasts (Fig. 4H and I). These results were further corroborated by colony bleaching of the L354 strain treated with LQA_78 (Fig. 4G), which differed from the partial inhibition of melanin production observed in the H99(NA) and (A) strains after LQA_78 treatment (Fig. 4A and D).

LQA_78 does not affect β -1,3-glucan, chitin, and chitosan content in the cell wall of *Cryptococcus neoformans*. LQA_78, at inhibitory concentration, did not significantly affect the cell wall components of *C. neoformans*. However, there was a slight reduction in the chitin content and increase in β -1,3-glucan and chitosan amount of the cell wall of LQA_78-treated yeasts compared to the untreated group (Fig. 5).

LQA_78 induces increased ROS production and *Cryptococcus neoformans* plasma membrane leading to cell death. The time-kill curve assay was performed with *C. neoformans* (H99[NA] and H99[A] strains) using different concentrations of LQA_78. At $2 \times \text{IC}_{50}$ and IC_{50} values, fungal growth was inhibited by about 90% and 50% after 24 h of treatment compared with the untreated yeasts. At higher LQA_78 concentrations (i.e., $4 \times$ and $8 \times \text{IC}_{50}$), induced cell death and no CFU were detected after 24 and 4 h of treatment, respectively (Fig. 6A and Fig. S4A).

In this regard, a significant increase in DNA and protein content was observed when yeasts from H99(NA) were treated with LQA_78 (Fig. S5A and B), while the DNA and proteins content of the supernatant from H99(A) was not significantly different from the untreated yeasts (Fig. S4C and D). This cytoplasm extravasation was associated with the increased plasma membrane permeability of the yeasts treated with LQA_78 ($4 \times \text{IC}_{50}$ and $8 \times \text{IC}_{50}$) since there was a significant increase in PI-positive cell percentage compared to the untreated group of both strains (Fig. 6B and Fig. S4B).

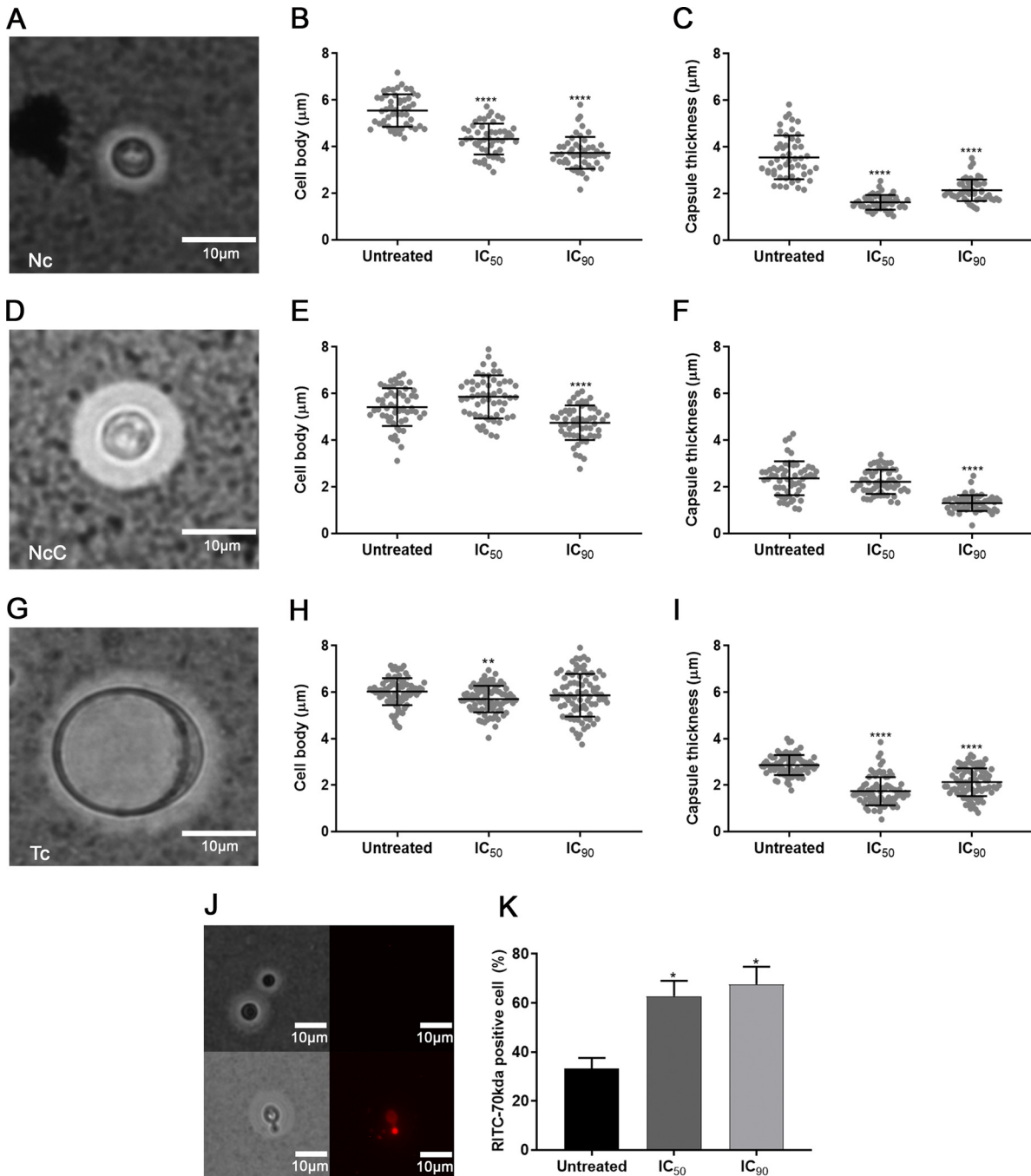


FIG 3 Inhibitory effect of LQA_78 on virulence factors of *Cryptococcus neoformans* H99. (A–I) India ink staining and morphometry of normal cells (Nc), normal cells with enlarged capsule (NcC), and titan cells (Tc). (J–K) Capsular permeability in NcC using rhodamine isothiocyanate-dextran 70 kDa (RITC-70kDa). *, $P < 0.05$; **, $P < 0.01$; and ****, $P < 0.0001$ compared with the untreated group of two independent experiments in duplicate (one-way ANOVA with Dunnett's posttest). $n = 50$ to 100 cells.

Furthermore, LQA_78 at concentrations $>IC_{50}$ values induced a significant increase in ROS production compared to the untreated group (Fig. 6C), and this effect may be associated with the loss of mitochondrial membrane potential (Fig. 6D).

LQA_078 delays the lethality of *Galleria mellonella* larvae infected with *Cryptococcus neoformans* by reducing the fungal burden and inhibiting capsule enlargement and titan cell formation. The toxic effect of LQA_78 using an invertebrate model of *G. mellonella* was not observed at a dose of 46.5 mg/kg; however, higher doses significantly reduced the larval survival (Fig. 7A).

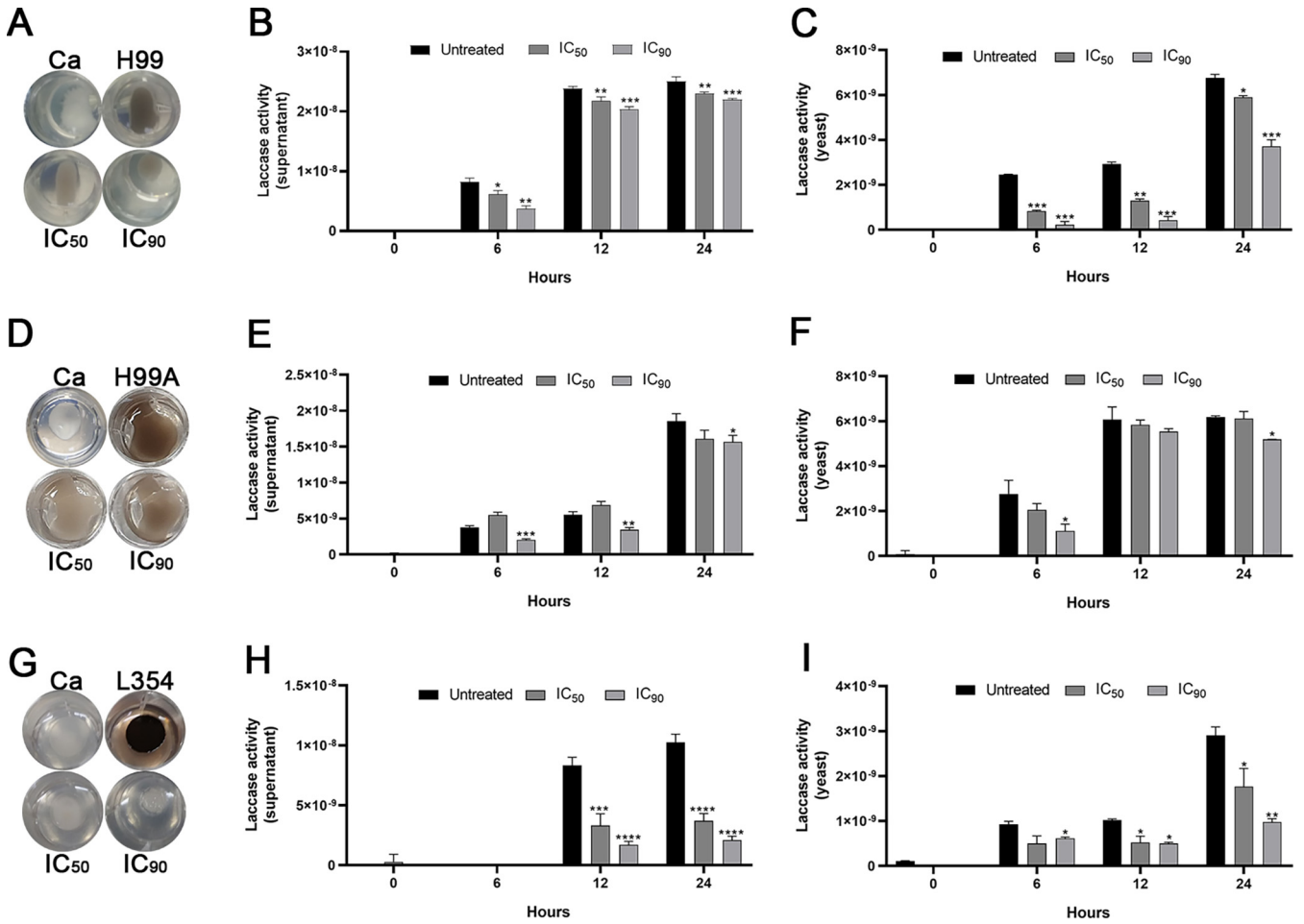


FIG 4 Inhibitory effect of LQA_78 on melanin production and laccase activity in *Cryptococcus neoformans* strains. The melanin was produced on agar after 48 h of incubation at 30°C (A, D, G) and the laccase activity in the supernatant (B, E, H) and in the yeasts (C, F, I) was evaluated at different incubation times (0, 6, 12, and 24 h) at 30°C by measuring the optical density (OD) at 480 nm. (A–C) H99(NA), (D–F) H99(A), and (G–I) clinical isolate L354. *, $P < 0.05$; **, $P < 0.01$; ***, $P < 0.001$; and ****, $P < 0.0001$ compared with the untreated group of two independent experiments, in triplicate (B–C, E–F, H–I) and duplicate (A, D, G) (one-way ANOVA with Dunnett’s posttest). Ca, *Candida albicans*.

Compared to the untreated group, AMB or LQA_78 delayed the lethality of *C. neoformans* in *G. mellonella* larvae. AMB (10 mg/kg) protected 30.6% of larvae 7 days after infection ($P < 0.001$). Although 100% of the larvae treated with LQA_78 (20 and 40 mg/kg) died 7 days postinfection, the compound afforded slight protection to the larvae at the beginning of infection compared to the untreated group ($P < 0.05$) (Fig. 7B).

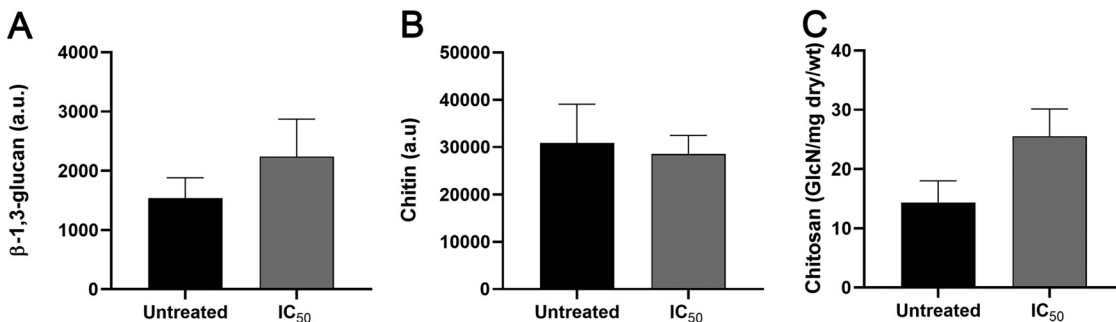


FIG 5 Effect of the LQA_78 on cell wall components of *Cryptococcus neoformans* H99. (A) β -1,3-glucan quantification, (B) chitin quantification, and (C) chitosan quantification. The assays were performed, in duplicate, in two independent experiments. Student’s *t* test was used to compare untreated and treated groups. wt, weight. a.u., arbitrary unit.

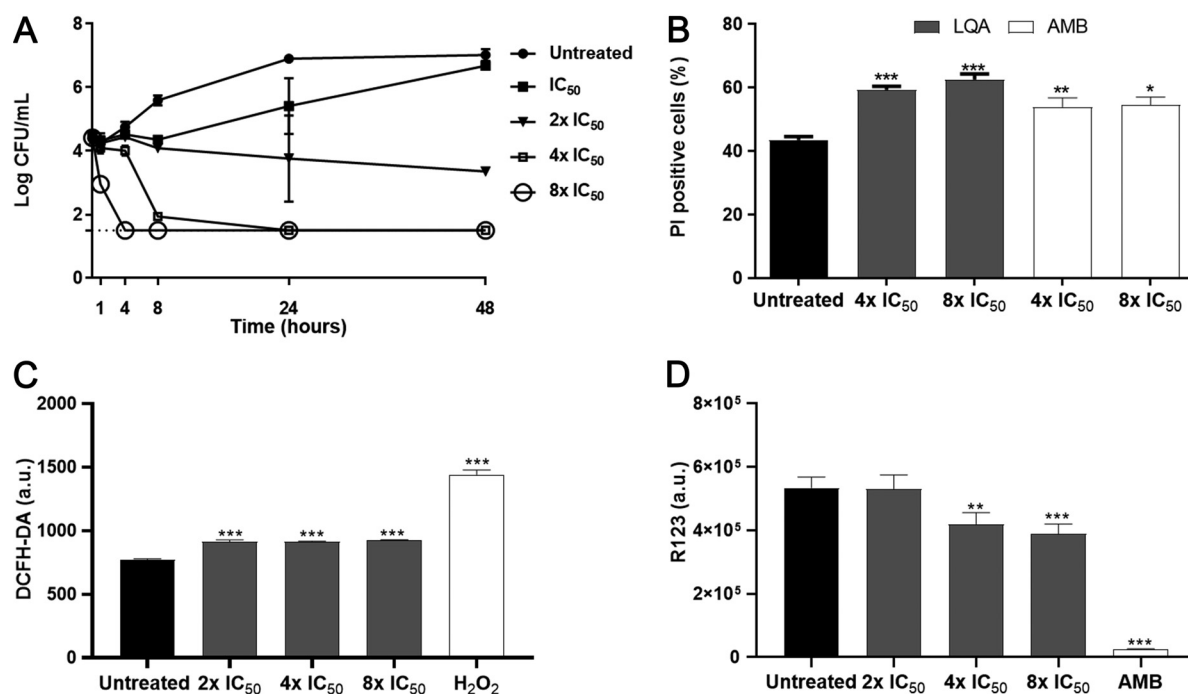


FIG 6 Fungicidal effect of LQA₇₈ on *Cryptococcus neoformans* H99. (A) The yeasts treated with several concentrations of LQA₇₈ (IC₅₀ = 4 μg/mL) were analyzed by CFU counting to determine the time-kill curve. (B–D) The yeasts treated with fungicidal concentrations for 24 h were analyzed by flow cytometry using propidium iodide (PI) for membrane permeability detection (B), 2',7'-dichlorofluorescein diacetate (DCFH-DA) for ROS quantification (C), and rhodamine 123 (R123) for mitochondrial membrane potential assessment (D). Hydrogen peroxide (H₂O₂) and amphotericin B (AMB) were used as controls for the assays. *, $P < 0.05$; **, $P < 0.01$; and ***, $P < 0.001$ compared with the untreated group (one-way ANOVA with Dunnett's posttest). Two independent experiments of the time-kill curve (in duplicate) and flow cytometry (in triplicate; 100,000 events/sample) were performed. a.u., arbitrary unit.

LQA₇₈ at 20 mg/kg led to a significant reduction in the fungal burden ($P < 0.05$) (Fig. 7C), inhibiting Tc formation and reducing capsule thickness compared to the untreated group (Fig. 7D and E). Furthermore, the compound significantly increased the number of total hemocytes in the hemolymph of the larvae compared to the noninjected (NI) group ($P < 0.05$). As expected, the number of hemocytes increased in the *C. neoformans*-infected larvae (Fig. 7F). However, larvae infected with H99 and treated with LQA₇₈ displayed reduced hemocyte counts (Fig. 7F), a phenomenon possibly associated with infection control by the compound.

DISCUSSION

Twenty-seven synthetic quinoline compounds were screened for *in vitro* antifungal activity and red blood cell cytotoxicity. Eleven compounds exhibited an antifungal effect, mainly against *Cryptococcus*, and none of these compounds showed hemolytic activity. This observation is relevant because AMB, the first-choice drug for the induction CM treatment, has a reported hemolytic activity of 50% at ~17 μg/mL (6, 13). Additionally, the organoselenium-quinoline compound LQA₇₈ (compound 2) had notable inhibitory and fungicidal effects against *C. neoformans* and *C. albicans*. Thus, it was selected as the lead compound for conducting subsequent assays evaluating its anticryptococcal actions.

Although the antifungal activity of quinoline derivatives on yeasts and filamentous fungi has been described (14) at concentrations similar to ours, the quinoline core does not seem to be essential for the observed antifungal effect. Indeed, when the most active compound, LQA₇₈, was compared with its structural analog 26 (without Se and nonactive), the presence of the Se atom indicates that it is essential for antifungal action (Table S1). The side chain directly linked to the quinoline core also seems important since the comparison between the structural analogs showed that those with lower IC₅₀ values and fungicidal activity had a halogenated group (bromine-2,

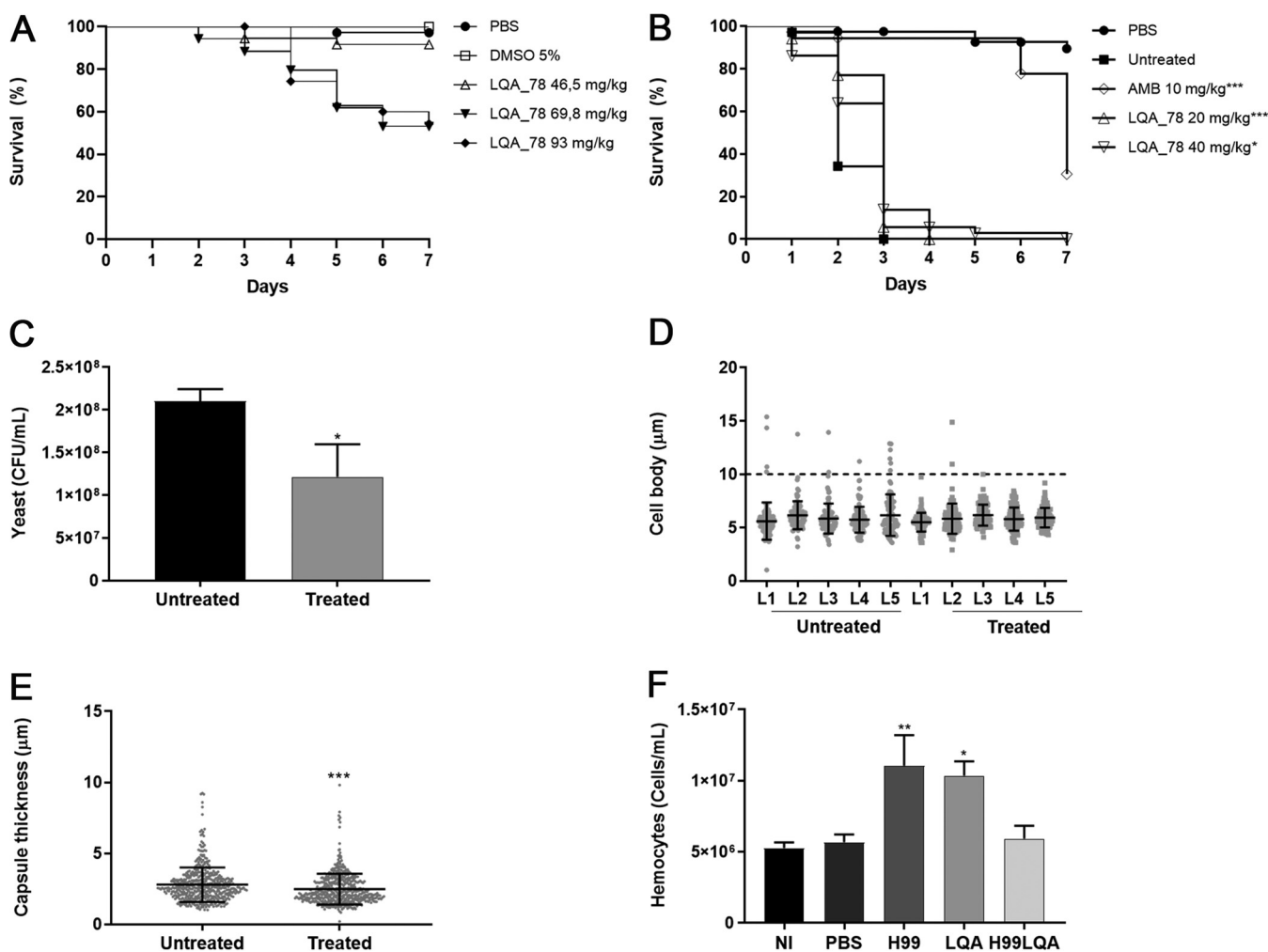


FIG 7 Toxicity and antifungal effect of LQA_78 on *Galleria mellonella* larval model. (A) LQA_78 toxicity by the survival curve analysis ($n = 20$ larvae/group). (B) Efficacy of LQA_78 treatment on the larvae infected with yeasts of *Cryptococcus neoformans* H99 by the survival curve analysis ($n = 20$ larvae/group). (C) CFU counting in the hemolymph 24 h postinfection ($n = 5$ larvae/group). (D–E) Titan cell formation and capsule thickness of yeasts in the hemolymph 24 h postinfection. (F) Total hemocyte counting in the hemolymph after 24 h of infection and/or treatment ($n = 5$ larvae/group). Statistical analyses were performed using Log-rank tests (Mantel-Cox) (A and B), t test (C and E), and one-way ANOVA with Dunnett's posttest (F). *, $P < 0.05$; **, $P < 0.01$; ***, $P < 0.001$; and ****, $P < 0.0001$ compared with the PBS group (A) or with the untreated/NI group (B–F) of two independent experiments.

chlorine-5, fluor-24, or iodine-25) (Table S1). Among these, the compound containing Br (compound 2 or LQA_78) was the most effective in inhibiting the growth of *C. neoformans* and *C. albicans* and presented fungicidal activity.

Recent approaches using organoselenium compounds, e.g., ebselen (EbSe) and diphenyl diselenide ([PhSe]₂), for studies of new antifungal agents against pathogenic fungi, have been reported (10). Herein, the organoselenium LQA_78 inhibited the fungal growth at concentrations ranging from 1 to 32 $\mu\text{g}/\text{mL}$ against *C. neoformans* (standard and clinical strains), leading to a significant increase in the budding formation and arresting yeasts in the G₂/M phase of the cell cycle. It has been reported that cell wall composition and integrity are important to the division/growth, morphogenesis, and virulence of *C. neoformans* yeasts (15). However, no significant alterations in the cell wall components (chitin, chitosan, and β -1,3-glucan) were observed in the yeasts treated with inhibitory LQA_78 concentrations. In addition, chitinases in *C. neoformans* are involved in bud separation (16), but the accumulation of budding yeasts caused by LQA_78 was not associated with an interference with chitinase activity.

The antifungal activity of LQA_78 seems unaffected by the triazole-resistance mechanisms described in *Cryptococcus*, which are associated with the overexpression of efflux pumps (*AFR1*, *AFR2*, *MDR1*, and *PDR11*) and *ERG11* (17, 18). Indeed, *C. neoformans*

H99(A), a tebuconazole-adapted strain, which expresses some of these resistance mechanisms (19), was also susceptible to LQA_78 with IC and minimum fungicidal concentration (MFC) values equivalent to the values obtained for the H99(NA), a non-adapted strain. Studies evaluating other organoselenium compounds reported IC values in the concentration range at or above those presented here (10, 20).

LQA_78 displayed substantial fungicidal action against *C. neoformans*. This effect may be associated with increased plasma membrane permeability due to higher proteins and DNA extravasation levels and more PI-labeled cells. The plasma membrane permeabilization by ROS is a well-known mechanism for several fungicidal drugs, e.g., AMB and miltefosine, since intracellular accumulation inflicts membrane damage and causes cell death (21, 22). Our work revealed that fungicidal concentrations of LQA_78 increased ROS levels and significantly reduced the mitochondrial membrane potential in yeasts. Previous studies reported that EbSe and (PhSe)₂ act on the fungal redox system, depleting glutathione (GSH), or inhibiting thioredoxin reductase (TrxR) through covalent interactions between the Se atom and a cysteine residue in *Cryptococcus* and *A. fumigatus*, leading to augmented ROS production and cell structure and lipid membrane damage (20, 23). Furthermore, efflux pumps and ATPase of plasma membranes were reported as targets for chalcogenides compounds that impair fungal growth and virulence (20, 24).

Inhibiting *Cryptococcus* virulence factors may be a strategy that contributes to the effectiveness of antifungal therapies. In addition to the fungicidal effect, LQA_78 also inhibits cells from biofilms, melanin production, capsule enlargement, and *Cryptococcus* morphotypes. These factors represent fungal weapons that contribute to immune system escape mechanisms, successful infection and spread to the host's central nervous system.

Concerning biofilms, they are associated with persistent infections, leading to high fungal resistance to the host's immune mechanisms and antifungal therapy (25). Although LQA_78 did not inhibit the sessile cells from mature *C. neoformans* biofilms, it attenuated dispersed cell growth. This inhibition is extremely important in controlling the infection, preventing the formation and spread of new biofilm sites, and the emergence of cells less susceptible to antifungals (26).

The melanin produced during the infection is another factor that reduces the *Cryptococcus* susceptibility to traditional antifungals and immune response. This pigment is deposited on the cell wall, a process that is strongly influenced by chitosan content, which is responsible for retaining melanin (27). However, the yeasts treated with the LQA_78 did not show significant changes in cell wall components (β -1,3-glucan, chitin, and chitosan), and we did not observe any leak of melanin to the extracellular medium.

The presence of the melanin in cell wall contributes to ROS sequestration and reducing drug permeability (28). Interestingly, the organoselenium LQA_78, at inhibitory concentrations, attenuated fungal melanization by inhibiting laccase production in the yeasts and supernatant, resulting in suppressed enzyme activity for up to 24 h. This finding is due to the pretreatment of *C. neoformans* yeasts with the compound using an induction medium for laccase expression (glucose-free asparagine salt) (29). Among standard antifungals, only voriconazole has been reported to reduce *C. neoformans* melanin production (30).

Additionally, Tc formation and capsule enlargement are important for establishing fungal infection and dissemination. The Tc are resistant to phagocytosis and oxidative stress, which favor fungal survival in the lungs (31). Although this morphotype is restricted to the lungs, its presence in the host is associated with the increased dissemination of normal cells and microcells to the central nervous system (32), mainly via a Trojan horse mechanism (33).

The polysaccharide capsule is the main virulence factor of *Cryptococcus* because it offers protection to the fungus against the host's defense system (5). In this regard, thick capsules are less permeable than thin capsules resulting in increased resistance to oxidative stress and antifungals (12, 34). Moreover, during the intracellular phase, the capsule mitigates the microbicide response of macrophages (5, 12, 34). Here, LQA_78 inhibited the Tc and NcC growth and increased the capsule permeability impairing the fungal pathogenesis.

The *in vivo* *G. mellonella* larval model results corroborated the *in vitro* data. At doses considered safe (below 46.5 mg/kg), in addition to inhibiting Tc formation and reducing the capsule thickness of *C. neoformans* yeasts during infection, LQA_78 significantly decreased the fungal burden. Interestingly, LQA_78 had an immunomodulatory effect, stimulating the increase of total hemocytes in the hemolymph of the larva. This immunomodulatory effect was also observed for other antifungals, such as caspofungin, which increases hemocytes in larval hemolymph (35), and AMB, which stimulates the production of cytokines and other immune system components (36). Although LQA_78 displayed high cytotoxicity against four mammalian cell lineages, the antivirulence effects, fungicidal and immunomodulatory actions of LQA_78 indicate that this compound could be used as a lead molecule for the development of antifungal drugs with improved safety and effectiveness for controlling *C. neoformans* infections.

In conclusion, the organoselenium LQA_78 inhibited *C. neoformans* growth, arresting yeast in the G₂/M phase, and displayed antivirulence effects, such as inhibiting dispersed biofilm cells, Tc, and NcC, and melanin and capsule production. Additionally, LQA_78 exhibited fungicidal action, inducing ROS production, and consequently increasing plasma membrane permeability. Using the larval model of *G. mellonella*, antifungal and immunomodulatory effects were observed. These promising results encourage us to set more ambitious goals to improve the LQA_78 compound. Subsequent iterations of this potential lead compound could provide a glimpse into the future of cryptococcosis treatment.

MATERIALS AND METHODS

Microorganisms. *Aspergillus fumigatus* ATCC 16913, *Candida albicans* SC 5314, and *Cryptococcus neoformans* H99 (called nonadapted [NA] strain) were used to screen 27 compounds containing a quinoline core for antifungal activity. *C. neoformans* H99 adapted to tebuconazole (A strain), which displays cross-resistant to clinical azole agents (17), was also employed. Additionally, *C. neoformans* CAP59 (H99 a capsular mutant) (37) and 14 previously identified human clinical isolates (38) were used.

The fungi were kept in brain and heart infusion broth with 20% glycerol at -80°C and recovered on Sabouraud dextrose agar (SDA, Becton, Dickinson, Sparks, MD, USA) at 35°C . Before each assay, fungi were subcultured twice in the same medium for 48 to 72 h at 35°C .

Antifungal drugs. Fluconazole (FLC) and amphotericin B (AMB) (both from Sigma-Aldrich, St. Louis, MO, USA) were dissolved in dimethyl sulfoxide (DMSO, Vetec, St. Louis, MO, USA) and stored at -20°C as stock solutions at concentrations at least 100 times higher than the highest concentration used (e.g., 2,560 $\mu\text{g}/\text{mL}$ FLC and 1,600 $\mu\text{g}/\text{mL}$ AMB) (39, 40).

Synthetic compounds. The 27 quinoline core compounds with and without selenium (Se) (1–27) were synthesized as previously described (41) (Fig. 1). The powders and stock solutions in DMSO were aliquoted and stored at -80°C . The final concentration of DMSO in the work solution was $\leq 5\%$.

Antifungal activity. The inhibitory effect of compounds was assessed on *A. fumigatus* ATCC 16913, *C. albicans* SC5314, and *C. neoformans* H99(NA) using the broth microdilution technique (39, 40) to select the most active molecule. The selected compound and standard antifungals were tested against H99(A), CAP59, and clinical isolates of *C. neoformans*. The lowest concentrations that inhibit fungal growth by 50% and 90% (IC₅₀ and IC₉₀, respectively) were visually determined after incubation for 48 h at 35°C . *Candida parapsilosis* ATCC 22019 was used as a quality control strain in the assay. The criteria of interpretation for standard antifungals were based on (11).

Minimum fungicidal concentration (MFC), defined as the lowest concentration of the compound able to reduce the cell viability by $>99.9\%$, was also determined. Compounds were considered fungicidal if the MFC value was equal to or 4 times greater than the IC₉₀ (42).

Checkerboard assay. Combining compound LQA_78 with FLC or AMB on *C. neoformans* H99 (NA and A strains) was performed using the checkerboard technique (43). The interaction profile between LQA_78 and FLC or AMB was evaluated after calculating the Fractional Inhibitory Concentration Index (FICI) (44).

Hemolytic activity. A suspension of 4% sheep red blood cells (Newprovi, Pinhais, Paraná, Brazil) (vol/vol, in a 5% sterile glucose solution) was treated with compounds that inhibit fungal growth at IC₅₀ $\leq 16 \mu\text{g}/\text{mL}$ for 2 h in a water bath at 37°C . Negative (untreated) and positive (0.1% Triton X-100, Sigma-Aldrich) controls were also included for hemolytic activity (HA) determination (45).

Compound 2 (or LQA_78) exhibited the lowest IC values, substantial fungicidal activity, and a low hemolytic effect and was selected for further antifungal characterization against *C. neoformans* H99(NA), H99(A), and L354 (clinical isolate).

Cytotoxicity assay. HCT116 (colon adenocarcinoma, ATCC 247), MCF7 (breast adenocarcinoma, ATCC HTB-22) and CCD-18Co (nontumoral colon fibroblasts, ATCC CRL-1459) cells were obtained from the American Type Culture Collection (ATCC). The macrophages J774A.1 were kindly provided by Niels Olsen Saraiva Câmara (Institute of Biomedical Sciences, USP). Cell culture conditions were developed using the Roswell Park Memorial Institute (RPMI) medium for HCT116, Dulbecco's modified Eagle's medium (DMEM) for MCF7 and J774A.1, and Eagle's minimum essential medium (EMEM) for CCD-18Co, supplemented with 10% fetal bovine serum (FBS) and 1% penicillin-streptomycin. For J774A.1 culture, the medium was supplemented

with 2-mercaptoethanol (0.05 mM) (all reagents were purchased from Thermo Fisher Scientific, San Jose, CA, USA). Cells were kept in a humidified atmosphere with 5% CO₂ at 37°C.

A suspension of 6×10^3 cells/well was added to wells of 96-well plates, and the plates were incubated for 24 h. Then, the cell monolayer was treated with LQA_78 (0.0064 to 100 µg/mL) for 72 h at 37°C and 5% CO₂. Finally, cell viability was analyzed by the 3-(4,5-dimethylthiazol-2-yl)-2,5-diphenyltetrazolium bromide (MTT, Thermo Fisher Scientific) reduction method to determine the cytotoxic concentration of the 50% (CC₅₀) and 95% confidence interval (CI95%) by sigmoidal nonlinear regression (46). The selectivity index (SI) of LQA_78 was determined by the CC₅₀ and IC₅₀ median ratio.

Effect on *Cryptococcus neoformans* budding. After the broth microdilution assay, yeasts of *C. neoformans* (H99[NA], H99[A], and L354) treated with IC₅₀ and IC₉₀ concentrations of LQA_78 were visualized under a light microscope. Yeasts with and without budding were counted (100 to 250 cells from 1.0 to 2.5×10^6 CFU/mL) using a Neubauer chamber and compared to untreated yeasts.

Antifungal activity on mature *Cryptococcus neoformans* biofilms. The activity of LQA_78 or AMB was evaluated on sessile and dispersed cells from mature biofilms. *C. neoformans* (H99[NA], H99[A], and L354) were standardized to 1×10^7 CFU/mL in RPMI 1640 medium with 0.16 M MOPS. Then, 100 µL was added to the wells of 96-well flat-bottom plates and incubated (without agitation) at 35°C for 48 h for biofilm formation (47).

After incubation, the dispersed cells present in the supernatant were collected to assess the susceptibility test to LQA_78 or AMB (39). The sessile cells were washed twice with PBS and treated with LQA_78 or AMB for 48 h at 35°C (without agitation). Then, the wells were washed with PBS and the metabolic activity of the biofilm cells was determined by the 2,3-bis (2-methoxy-4-nitro-5-sulphophenyl)-2H-tetrazolium-5-carboxanilide (XTT, Sigma-Aldrich) reduction method (25). The lowest concentrations inhibiting 50% and 90% of fungal growth (BIC₅₀ and BIC₉₀, respectively) of dispersed cells and metabolic activity of sessile cells from biofilms were determined.

Antifungal activity on *Cryptococcus neoformans* morphotypes. The antifungal effect of LQA_78 was also assessed on two morphotypes of *C. neoformans* (H99[NA], H99[A], and L354), normal cells with enlarged capsule thickness (NcC), and titan cells (Tc), using the broth microdilution assay. The IC and MFC values were compared to normal cells (Nc).

The Nc cells were obtained after growth on SDA for 72 h at 37°C. Nc were then cultivated in an artificial cerebrospinal fluid (ACSF) for 72 h at 37°C, with agitation at 150 rpm to induce the capsule enlargement (i.e., NcC) (48).

Tc cells (diameter of the cell body ≥ 10 µm) were obtained by incubating Nc in yeast nitrogen base (YNB) broth for 24 h at 37°C, with agitation at 150 rpm, adjusting the inoculum to 1×10^6 CFU/mL in PBS plus 10% FBS and incubating in microaerophilia at 37°C for 72 h with under agitation at 150 rpm (49).

Light microscopy analysis of capsule thickness and cell body diameter of *Cryptococcus neoformans* morphotypes. The cell morphotypes (Nc, NcC, and Tc) of *C. neoformans* (H99[NA], H99[A], and L354) untreated and treated with IC₅₀ and IC₉₀ values of LQA_78 were visualized using India ink staining under light microscopy, and the images were captured (EVOS FL, Thermo Fisher Scientific). For each morphotype, 50 to 100 cells were analyzed using the ImageJ 1.49v program (<https://imagej.nih.gov/ij>). The capsule thickness measurement was defined as the difference between the total cell diameter (including capsule) and the cell body diameter (defined by the cell wall) (19).

Analysis of capsular permeability. The NcC cells (1×10^7 CFU/mL) of *C. neoformans* (H99[NA], H99[A], and L354) in ACSF were treated with LQA_78 (IC₅₀ and IC₉₀) for 48h at 35°C. The untreated and treated yeasts were washed twice in PBS, and a mix of rhodamine isothiocyanate dextran 70 kDa (RITC-70kDa, Sigma-Aldrich), at 16 µg/mL in ethanol, with India ink was added for visualization by light and fluorescence microscopy and determination of the percentage of labeled cells (12).

Inhibition of cryptococcal melanization. Minimum medium (15 mM dextrose, 10 mM MgSO₄, 29.4 mM KH₂PO₄, 13 mM glycine, 3 µM thiamine-HCl, with or without 1.5% agar) was prepared with 1 mM L-3,4-dihydroxyphenylalanine (L-DOPA) (Sigma-Aldrich) to induce melanization in *C. neoformans* (H99[NA], H99[A], and L354). LQA_78 (4 and 8 µg/mL) and 20 µL of the fungal inoculum (1×10^6 CFU/mL) were added to the medium and incubated in a dark, humid chamber for 48 to 72 h at 35°C (50). *C. albicans* SC5314 was used as the negative control for melanization. Additionally, the melanin in the supernatant was detected by optical density measurement at 480 nm (29).

LQA_78 assessment on laccase activity. Yeasts of *C. neoformans* (H99[NA], H99[A], and L354) were grown in 5 mL of yeast extract peptone dextrose (YEPD) at 30°C for 24 h. Then, the yeasts were collected by centrifugation at $1,000 \times g$ for 10 min and grown in 5 mL of asparagine salt (0.3% glucose, 0.1% L-asparagine, 0.05% MgSO₄, 1% of solution 1 M Na₂HPO₄ [pH 6.5], 3 µM thiamine, 0.001% of solution 0.5 M CuSO₄) for 5 days for 30°C with agitation at 200 rpm. Yeasts were washed with 50 mM Na₂HPO₄ (pH 7.0) and, subsequently, adjusted to 1×10^7 CFU/mL in glucose-free asparagine salt to induce laccase expression for 72 h at 30°C and with agitation at 200 rpm (untreated yeasts). In addition, the fungal inoculum was treated with LQA_78 (IC₅₀ and IC₉₀) under the same conditions as untreated yeasts for further evaluation of laccase activity in the supernatant and yeasts.

Laccase secretion in the supernatant was normalized by the number of total yeasts at the end of the culture (laccase/yeast). Then, each sample was centrifuged ($4,000 \times g$ for 5 min), and 180 µL of the supernatant and 20 µL of L-DOPA (10 mM) were added to the 96-well plate in triplicate. In addition, 450 µL of yeasts previously treated or not with LQA_78, at 1×10^7 CFU/mL in glucose-free asparagine salt, were mixed with 50 µL of L-DOPA (10 mM) in wells of 24-well plates in duplicate. Volumes of 200 µL of supernatant and 500 µL and fungal suspension were included as laccase activity blank and the same volume of L-DOPA alone was used as a control. Finally, melanin production was evaluated at different

incubation times (0, 6, 12, and 24 h) at 30°C by measuring the optical density (OD) at 480 nm. Laccase activity was calculated using the following formula (29):

$$\text{Laccase activity } (\mu\text{mol/yeast number}) = \text{OD mean}/(7.9 \times \text{number yeast in the culture})$$

Time-kill curve. *C. neoformans* H99 (NA and A strains) were standardized to 5×10^4 CFU/mL, exposed to different concentrations of LQA_78 (IC_{50} to $8 \times \text{IC}_{50}$) in RPMI 1640 medium buffered with 0.16 M MOPS and incubated at 35°C. After 1, 4, 8, 24, and 48 h of incubation, the yeasts were serially diluted (1:10), plated on SDA, and incubated for 72 h at 35°C. The CFU were counted to construct the time-kill curves (51).

Plasma membrane permeability. *C. neoformans* H99 (NA and A strains) were standardized to 1×10^7 CFU/mL and exposed to IC_{50} to $4 \times \text{IC}_{50}$ concentrations of LQA_78 diluted in PBS. Untreated yeasts were used as the control for cell membrane integrity. After 1, 4, 8, and 24 h of incubation at 35°C, the supernatant was collected by centrifugation for 8 min at $13,000 \times g$, and the absorption at 260 nm (DNA) and 280 nm (protein) was measured in a Nanodrop 2000 spectrophotometer (Thermo Fisher Scientific).

Flow cytometry analyses. *C. neoformans* H99(NA) standardized to 1×10^7 CFU/mL was exposed to LQA_78 ($2 \times \text{IC}_{50}$ to $8 \times \text{IC}_{50}$), AMB (1 $\mu\text{g/mL}$), or H_2O_2 (50 μM), and diluted in PBS for 24 h at 35°C. Then, the yeasts were collected, washed with cold PBS, adjusted to 1×10^6 CFU/mL, and labeled with 5 $\mu\text{g/mL}$ propidium iodide (PI, Invitrogen) (plasma membrane permeability), 5 $\mu\text{g/mL}$ rhodamine 123 (Sigma-Aldrich) (mitochondrial membrane potential), or 40 $\mu\text{g/mL}$ 2'7'-dichlorofluorescein diacetate (DCFH-DA, Sigma-Aldrich) (ROS production) for 30 min and at room temperature in a dark chamber (22).

For analyses of the cell cycle and cell wall components, *C. neoformans* H99(NA) yeasts at 1×10^3 CFU/mL treated with LQA_78 for 48 h at 35°C were fixed with 4% formaldehyde for 30 min, washed in cold PBS, and permeabilized with 0.1% Triton X-100 for 30 min at room temperature. Finally, the yeasts were adjusted to 1×10^6 CFU/mL, washed with PBS and labeled with 5 $\mu\text{g/mL}$ PI for 30 min in the dark at room temperature for cell cycle analysis (14) or with calcofluor White M2R (25 $\mu\text{g/mL}$, Sigma-Aldrich) and aniline blue (25 $\mu\text{g/mL}$, Sigma-Aldrich), for total quantification of chitin and β -1,3-glucan, respectively (52).

A sampling of 10,000 to 100,000 events was analyzed by flow cytometry using a BD Accuri C6 instrument (Becton, Dickinson, Sparks, MD, USA). The data were processed using the BD Accuri C6 software.

Cell wall chitosan measurement. To assess the chitosan content, we used the 3-methyl-2-benzothiazolinone hydrazone (MBTH) chemical method (53). Briefly, *C. neoformans* H99(NA) yeasts at 1×10^3 CFU/mL treated or not with LQA_78 (IC_{50}) for 48 h at 35°C in RPMI 1640 medium were harvested, washed in PBS, frozen, and freeze-dried. The dry weight was determined, and the pellet was suspended in 10 mL of 6% KOH and incubated in a water bath at 80°C for 60 min. Then, the samples were washed in ultrapure water, adjusted to a final concentration of 10 mg/mL and sonicated (5 cycles of 60 s). A 100- μL aliquot (equivalent to 1 mg dry weight) was used to chitosan assessment and mixed with 100 μL of 1 M HCl with consecutive addition of 400 μL NaNO_2 (2.5%) and incubated for 15 min/25°C. Posteriorly, 200 μL (12.5%) of ammonium sulfamate was added slowly and incubated for 5 min/25°C, followed by addition of 200 μL MBTH (0.25%) for 30 min at 37°C. Finally, 200 μL FeCl_3 (0.5%) was added and incubated for 5 min/37°C. The sample was centrifuged at $12,000 \times g$ for 5 min and 200 μL of the supernatant was transferred to a 96-well plate for measurement of absorbance at 650 nm. The calibration curve was prepared using several concentrations of D-glucosamine hydrochloride ranging from 0 to 100 nM. The chitosan content was expressed in nanomoles of glucosamine per milligram of dry weight of yeasts.

LQA_78 assessment on chitinase activity. To evaluate whether the effects of LQA_78 involved the activity of chitinase, we first analyzed microscopically the distribution of chitin and chitooligomers (54). *C. neoformans* H99(NA) yeasts at 10^6 CFU/mL in 10% Sabouraud dextrose broth in MOPS (pH 7.0) were treated or not with LQA_78 (IC_{50}) for 24 h at 37°C. After, the yeasts were fixed with 4% paraformaldehyde and blocked with 1% bovine serum albumin (BSA) in PBS for 1 h at 37°C. Chitin and chitooligomers detection in the cell wall was performed using 25 μM calcofluor white and 5 $\mu\text{g/mL}$ wheat germ agglutinin-tetramethylrhodamine conjugate, respectively, for 30 min at 37°C, and the images were recorded with LasAF software (Leica) and processed with ImageJ.

We also checked the surface-associated activity of chitinase in untreated or drug-treated cryptococci (54). The yeasts were prepared as described above, but time points of 0 to 4 h of drug exposure were also evaluated. For determination of enzyme activity, 10^6 yeasts were suspended in 180 μL of 6 mM the chitinase substrate (4-methylumbelliferyl N-acetyl- β -D-glucosaminide) in phosphate-citrate buffer (40 mM sodium citrate, 88 mM sodium phosphate dibasic [pH 4.5]) and incubated for 1 h at 37°C. Then, the cells were removed by centrifugation and the supernatants (160 μL) were collected and transferred to a new tube. The reaction was stopped with 40 μL of 0.1 M glycine buffer (pH 10), and enzyme activity was measured on a fluorimeter (wavelength: 360 to 450 nm; Synergy H1 Hybrid Multi-Mode Reader, BioTek).

Toxicity and antifungal activity using the larval model of *Galleria mellonella*. *G. mellonella* larvae (1.5 to 2.0 cm in length and body weight of 110 to 116 mg) were treated with 10 μL of the compound (46.5 mg/kg, 69.8 mg/kg, or 93 mg/kg) using a Hamilton syringe to evaluate the toxic potential of LQA_78. These results were compared with control larvae that only received vehicle (PBS group).

For determining antifungal activity, larvae were infected with 10 μL of *C. neoformans* H99 yeasts (5×10^6 CFU/mL) in the left hemocoel. After 30 min, 10 μL of LQA_78 (20 mg/kg or 40 mg/kg) or AMB (10 mg/kg) were injected into the right hemocoel, and PBS was injected into the infected larvae (untreated group).

The larvae ($n = 20$ per group) were incubated at 37°C for 7 days for both assays. The survivors and their health status were assessed daily to construct the survival and morbidity curves, respectively (55, 56).

Viability and morphological analysis of yeast in the *Galleria mellonella* hemolymph. Hemolymph from untreated larvae and larvae treated with LQA_78 (20 mg/kg) for 24 h after yeast infection ($n = 5$ per group) was collected and added to a tube containing an equal volume of IPS (Insect Physiological Saline) buffer (12). The hemolymph was serially diluted, plated on SDA, and incubated for 72 h at 35°C for CFU counting. Additionally, as described above, the yeasts from hemolymph were observed using India ink staining to assess cell diameter and capsular thickness.

Determination of total hemocytes in the *Galleria mellonella* hemolymph. The larvae were separated into five groups ($n = 5$ animals/group): (i) noninjected (NI) group (i.e., noninfected and nontreated); (ii) PBS, which received 10 μ L of PBS twice; (iii) H99, which received 10 μ L of *C. neoformans* H99 (5×10^8 CFU/mL) and 10 μ L of PBS; (iv) LQA, that received 10 μ L of 20 mg/kg LQA_78 and 10 μ L of PBS; and (v) H99LQA, that received 10 μ L of *C. neoformans* H99 (5×10^8 CFU/mL) and 10 μ L of 20 mg/kg LQA_78. Thirty minutes elapsed between the injections in the right and left hemocoels. After 24 h, the larvae hemolymph was collected as described above, and total hemocytes were counted in a Neubauer chamber.

Statistical analysis. The data were analyzed using the GraphPad Prism v8.0 software (GraphPad Software Inc., La Jolla, CA), and a 95% confidence level was considered significant.

Ethical approval. Ethical approval was not required for this study.

Data availability. All data will be made available from the corresponding author upon request.

SUPPLEMENTAL MATERIAL

Supplemental material is available online only.

SUPPLEMENTAL FILE 1, PDF file, 0.65 MB.

ACKNOWLEDGMENTS

We thank Veridiana Munford for the technical support in the flow cytometry assays.

This study was supported by Fundação de Amparo à Pesquisa do Estado de São Paulo (FAPESP, 2021/01279-5, 2020/00295-4, and 2015/17177-6), Conselho Nacional de Desenvolvimento Científico e Tecnológico (CNPq, 405556/2018-7 and 302418/2018-0), and Coordenação de Aperfeiçoamento de Pessoal de Nível Superior (CAPES). A.L.D.D.F., C.d.C.S., and I.M.D.O. were FAPESP fellows (2017/15226-5, 2018/12149-2, and 2016/04289-3, respectively) and D.F.F.D.J. was a CAPES fellow (finance code 001). K.I. and L.V.C.-L. are research fellows of the CNPQ (303373/2019-9 and 308276/2021-3, respectively). M.L.R. is on leave from a position of Associate Professor at the Microbiology Institute of the Federal University of Rio de Janeiro. He is a recipient of a CNPq fellowship of scientific productivity. F.C.G.R. is a recipient of a fellowship sponsored by the National Institute of Science and Technology of Innovation in Diseases of Neglected Populations (INCT-IDPN).

D.F.F.D.J. and A.L.D.D.F. performed the experiments, analyzed the results, and wrote the manuscript. I.M.D.O. and H.A.S. synthesized the compounds. L.C.D.A. and L.V.C.-L. were responsible for the experimental design and data analysis of the cytotoxicity assays. D.d.A.S., R.W.B., and A.S.d.A.M. contributed to obtaining and characterizing the *C. neoformans* tebuconazole-adapted strain and clinical isolates. F.C.G.R. and M.L.R. performed the chitinase activity experiments. C.d.C.S. discussed and analyzed the results. K.I. designed the experiments, analyzed the data, and wrote and edited the manuscript. All authors read and approved the manuscript before publication.

We declare no conflicts of interest.

REFERENCES

- Rajasingham R, Smith RM, Park BJ, Jarvis JN, Govender NP, Chiller TM, Denning DW, Loyse A, Boulware DR. 2017. Global burden of disease of HIV-associated cryptococcal meningitis: an updated analysis. *Lancet Infect Dis* 17: 873–881. [https://doi.org/10.1016/S1473-3099\(17\)30243-8](https://doi.org/10.1016/S1473-3099(17)30243-8).
- Rakotoarivelo RA, Raberahona M, Rasamoelina T, Rabezanahary A, Rakotomalala FA, Razafinambinintsoa T, Bénet T, Vanhems P, Randria MdD, Romanò L, Cogliati M, Cornet M, Andrianarivelo MR. 2020. Epidemiological characteristics of cryptococcal meningoencephalitis associated with *Cryptococcus neoformans* var. Grubii from HIV-infected patients in Madagascar: a cross-sectional study. *PLoS Negl Trop Dis* 14:e0007984. <https://doi.org/10.1371/journal.pntd.0007984>.
- Soares EA, Lazera MdS, Wanke B, Faria MD, Soares EA, Coutinho ZF. 2019. Mortality by cryptococcosis in Brazil from 2000 to 2012: a descriptive epidemiological study. *PLoS Negl Trop Dis* 13:e0007596. <https://doi.org/10.1371/journal.pntd.0007596>.
- Fernandes KE, Brockway A, Haverkamp M, Cartera DA, Cuomo CA, van Ogtrop F, Perfect JR. 2018. Phenotypic variability correlates with clinical outcome in *Cryptococcus* isolates obtained from Botswanan HIV/AIDS patients. *mBio* 9:e02016-18. <https://doi.org/10.1128/mBio.02016-18>.
- Zaragoza O. 2019. Basic principles of the virulence of *Cryptococcus*. *Virulence* 10:490–501. <https://doi.org/10.1080/21505594.2019.1614383>.
- Mourad A, Perfect JR. 2018. Present and future therapy of *Cryptococcus* infections. *J Fungi* 4:79. <https://doi.org/10.3390/jof4030079>.
- Iyer KR, Revie NM, Fu C, Robbins N, Cowen LE. 2021. Treatment strategies for cryptococcal infection: challenges, advances and future outlook. *Nat Rev Microbiol* 19:454–466. <https://doi.org/10.1038/s41579-021-00511-0>.
- Zafar H, Altamirano DS, Ballou ER, Nielsen K. 2019. A titanic drug resistance threat in *Cryptococcus neoformans*. *Curr Opin Microbiol* 52:158–164. <https://doi.org/10.1016/j.mib.2019.11.001>.

9. Matada BS, Pattanashettar R, Yernale NG. 2021. A comprehensive review on the biological interest of quinoline and its derivatives. *Bioorg Med Chem* 32:115973. <https://doi.org/10.1016/j.bmc.2020.115973>.
10. Benelli JL, Poester VR, Munhoz LS, Melo AM, Trápaga MR, Stevens DA, Xavier MO. 2021. Ebselen and diphenyl diselenide against fungal pathogens: a systematic review. *Med Mycol* 59:409–421. <https://doi.org/10.1093/mmy/myaa115>.
11. Córdoba S, Isla MG, Szusz W, Vivot W, Altamirano R, Davel G. 2016. Susceptibility profile and epidemiological cut-off values of *Cryptococcus neoformans* species complex from Argentina. *Mycoses* 59:351–356. <https://doi.org/10.1111/myc.12479>.
12. García-Rodas R, Casadevall A, Rodríguez-Tudela JL, Cuenca-Estrella M, Zaragoza O. 2011. *Cryptococcus neoformans* capsular enlargement and cellular gigantism during *Galleria mellonella* infection. *PLoS One* 6:e24485. <https://doi.org/10.1371/journal.pone.0024485>.
13. Ishida K, de Castro RA, dos Santos LPB, Quintella LP, Lopes-Bezerra LM, Rozental S. 2015. Amphotericin B, alone or followed by itraconazole therapy, is effective in the control of experimental disseminated sporotrichosis by *Sporothrix brasiliensis*. *Med Mycol* 53:34–41. <https://doi.org/10.1093/mmy/myu050>.
14. Machado GRM, Diederich D, Ruaro TC, Zimmer AR, Lettieri Teixeira M, de Oliveira LF, Jean M, van de Weghe P, de Andrade SF, Baggio Gnoatto SC, Fuentefria AM. 2020. Quinolines derivatives as promising new antifungal candidates for the treatment of candidiasis and dermatophytosis. *Braz J Microbiol* 51:1691–1701. <https://doi.org/10.1007/s42770-020-00348-4>.
15. Oliveira HC, Rossi SA, García-Barbazán I, Zaragoza O, Trevijano-Contador N. 2021. Cell wall integrity pathway involved in morphogenesis, virulence and antifungal susceptibility in *Cryptococcus neoformans*. *J Fungi* 7:831. <https://doi.org/10.3390/jof7100831>.
16. Rodrigues J, Ramos CL, Frases S, Godinho RMC, Fonseca FL, Rodrigues ML. 2018. Lack of chitin synthase genes impacts capsular architecture and cellular physiology in *Cryptococcus neoformans*. *Cell Surf* 2:14–23. <https://doi.org/10.1016/j.tcsv.2018.05.002>.
17. Basso LR, Gast CE, Bruzual I, Wong B. 2015. Identification and properties of plasma membrane azole efflux pumps from the pathogenic fungi *Cryptococcus gattii* and *Cryptococcus neoformans*. *J Antimicrob Chemother* 70:1396–1407. <https://doi.org/10.1093/jac/dku554>.
18. Sykes JE, Hodge G, Singapurri A, Yang ML, Gelli A, Thompson GR. 2017. In vivo development of fluconazole resistance in serial *Cryptococcus gattii* isolates from a cat. *Med Mycol* 55:396–401. <https://doi.org/10.1093/mmy/myw104>.
19. Bastos RW, Silva C, Neves V, Rocha M, José G, Freitas C, Costa C, Ferreira F, Dutra S. 2018. Environmental triazole induces cross-resistance to clinical drugs and affects morphophysiology and virulence. *Antimicrob Agents Chemother* 62:e01179–17. <https://doi.org/10.1128/AAC.01179-17>.
20. Thangamani S, Eldesouky HE, Mohammad H, Pascuzzi PE, Avramova L, Hazbun TR, Seleem MN. 2017. Ebselen exerts antifungal activity by regulating glutathione (GSH) and reactive oxygen species (ROS) production in fungal cells. *Biochim Biophys Acta Gen Subj* 1861:3002–3010. <https://doi.org/10.1016/j.bbagen.2016.09.029>.
21. Ferreira GF, Baltazar L de M, Alves Santos JR, Monteiro AS, Fraga LdO, Resende-Stoianoff MA, Santos DA. 2013. The role of oxidative and nitrosative bursts caused by azoles and amphotericin B against the fungal pathogen *Cryptococcus gattii*. *J Antimicrob Chemother* 68:1801–1811. <https://doi.org/10.1093/jac/dkt114>.
22. Spadari CC, Vila T, Rozental S, Ishida K. 2018. Miltefosine has a postantifungal effect and induces apoptosis in *Cryptococcus* yeasts. *Antimicrob Agents Chemother* 62:e00312–18. <https://doi.org/10.1128/AAC.00312-18>.
23. Marshall AC, Kidd SE, Lamont-Friedrich SJ, Arentz G, Hoffmann P, Coad BR, Bruning JB. 2019. Structure, mechanism, and inhibition of *Aspergillus fumigatus* thioredoxin reductase. *Antimicrob Agents Chemother* 63:e02281–18. <https://doi.org/10.1128/AAC.02281-18>.
24. Billack B, Santoro M, Lau-Cam C. 2009. Growth inhibitory action of ebselen on fluconazole-resistant *Candida albicans*: role of the plasma membrane H⁺-ATPase. *Microb Drug Resist* 15:77–83. <https://doi.org/10.1089/mdr.2009.0872>.
25. Martinez LR, Casadevall A. 2015. Biofilm Formation by *Cryptococcus neoformans*. *Microbiol Spectr* 3. <https://doi.org/10.1128/microbiolspec.MB-0006-2014>.
26. Uppuluri P, Lopez-Ribot JL. 2016. Go forth and colonize: dispersal from clinically important microbial biofilms. *PLoS Pathog* 12:e1005397. <https://doi.org/10.1371/journal.ppat.1005397>.
27. Chrissian C, Camacho E, Fu MS, Prados-Rosales R, Chatterjee S, Cordero RUB, Lodge JK, Casadevall A, Stark RE. 2020. Melanin deposition in two *Cryptococcus* species depends on cell-wall composition and flexibility. *J Biol Chem* 295:1815–1828. <https://doi.org/10.1074/jbc.RA119.011949>.
28. Jacobson ES, Ikeda R. 2005. Effect of melanization upon porosity of the cryptococcal cell wall. *Med Mycol* 43:327–333. <https://doi.org/10.1080/13693780412331271081>.
29. Sousa HR, Oliveira GP, Frazão SO, Gorgonha KCM, Rosa CP, Garcez EM, Junior JL, Correia AF, Freitas WF, Borges HM, Alves LGB, Paes HC, Trilles L, Lazera MS, Teixeira MM, Junior VLP, Felipe MSS, Casadevall A, Silva-Pereira I, Albuquerque P, Nicola AM. 2022. Faster *Cryptococcus* melanization increases virulence in experimental and human cryptococcosis. *J Fungi* 8:393. <https://doi.org/10.3390/jof8040393>.
30. Martinez LR, Ntiamoah P, Gácsér A, Casadevall A, Nosanchuk JD. 2007. Voriconazole inhibits melanization in *Cryptococcus neoformans*. *Antimicrob Agents Chemother* 51:4396–4400. <https://doi.org/10.1128/AAC.00376-07>.
31. Crabtree JN, Okagaki LH, Wiesner DL, Strain AK, Nielsen JN, Nielsen K. 2012. Titan cell production enhances the virulence of *Cryptococcus neoformans*. *Infect Immun* 80:3776–3785. <https://doi.org/10.1128/IAI.00507-12>.
32. Zaragoza O, Nielsen K. 2013. Titan cells in *Cryptococcus neoformans*: cells with a giant impact. *Curr Opin Microbiol* 16:409–413. <https://doi.org/10.1016/j.mib.2013.03.006>.
33. Santiago-Tirado FH, Onken MD, Cooper JA, Klein RS, Doering TL. 2017. Trojan horse transit contributes to blood-brain barrier crossing of a eukaryotic pathogen. *mBio* 8:e02183-16. <https://doi.org/10.1128/mBio.02183-16>.
34. Zaragoza O, Chrisman CJ, Castelli MV, Frases S, Cuenca-Estrella M, Rodríguez-Tudela JL, Casadevall A. 2008. Capsule enlargement in *Cryptococcus neoformans* confers resistance to oxidative stress suggesting a mechanism for intracellular survival. *Cell Microbiol* 10:2043–2057. <https://doi.org/10.1111/j.1462-5822.2008.01186.x>.
35. Kelly J, Kavanagh K. 2011. Caspofungin primes the immune response of the larvae of *Galleria mellonella* and induces a non-specific antimicrobial response. *J Med Microbiol* 60:189–196. <https://doi.org/10.1099/jmm.0.025494-0>.
36. Mesa-Arango AC, Scorzoni L, Zaragoza O. 2012. It only takes one to do many jobs: amphotericin B as antifungal and immunomodulatory drug. *Front Microbiol* 3:286. <https://doi.org/10.3389/fmicb.2012.00286>.
37. Moyrand F, Janbon G. 2004. UGD1, encoding the *Cryptococcus neoformans* UDP-glucose dehydrogenase, is essential for growth at 37°C and for capsule biosynthesis. *Eukaryot Cell* 3:1601–1608. <https://doi.org/10.1128/EC.3.6.1601-1608.2004>.
38. Ponzio V, Chen Y, Rodrigues AM, Tenor JL, Toffaletti DL, Medina-Pestana JO, Colombo AL, Perfect JR. 2019. Genotypic diversity and clinical outcome of cryptococcosis in renal transplant recipients in Brazil. *Emerg Microbes Infect* 8:119–129. <https://doi.org/10.1080/22221751.2018.1562849>.
39. Clinical and Laboratory Standards Institute. 2017. Reference method for broth dilution antifungal susceptibility testing of yeasts. 4th ed. CLSI, Wayne, PA.
40. Clinical and Laboratory Standards Institute. 2017. Reference method for broth dilution antifungal susceptibility testing of filamentous fungi. 3rd ed. CLSI, Wayne, PA.
41. Oliveira IM, Vasconcelos SSN, Barbeiro CS, Correra TC, Shamim A, Pimenta DC, Caracelli I, Zukerman-Schpector J, Stefani HA, Manarin F. 2017. Ytterbium(III)-catalyzed three-component reactions: synthesis of 4-organoselenium-quinolines. *New J Chem* 41:9884–9888. <https://doi.org/10.1039/C7NJ01803G>.
42. Pfaller MA, Messer SA, Boyken L, Hollis RJ, Rice C, Tendolcar S, Diekema DJ. 2004. In vitro activities of voriconazole, posaconazole, and fluconazole against 4,169 clinical isolates of *Candida* spp. and *Cryptococcus neoformans* collected during 2001 and 2002 in the ARTEMIS global antifungal surveillance program. *Diagn Microbiol Infect Dis* 48:201–205. <https://doi.org/10.1016/j.diagmicrobio.2003.09.008>.
43. Pillai SK, Moellering RC, Eliopoulos GM. 2005. Antimicrobial combinations, p 365–440. In Lorian V (ed), *Antibiotics in Laboratory Medicine*, 5th ed, The Lippincott Williams & Wilkin Co, Philadelphia, PA.
44. Odds FC. 2003. Synergy, antagonism, and what the checkerboard puts between them. *J Antimicrob Chemother* 52:1. <https://doi.org/10.1093/jac/dkg301>.
45. Spadari CC, de Bastiani FdS, Lopes LB, Ishida K. 2019. Alginate nanoparticles as non-toxic delivery system for miltefosine in the treatment of candidiasis and cryptococcosis. *Int J Nanomed* 14:5187–5199. <https://doi.org/10.2147/IJN.S205350>.
46. Mosmann T. 1983. Rapid colorimetric assay for cellular growth and survival: application to proliferation and cytotoxicity assays. *J Immunol Methods* 65:55–63. [https://doi.org/10.1016/0022-1759\(83\)90303-4](https://doi.org/10.1016/0022-1759(83)90303-4).

47. Martinez LR, Casadevall A. 2006. Susceptibility of *Cryptococcus neoformans* biofilms to antifungal agents in vitro. *Antimicrob Agents Chemother* 50:1021–1033. <https://doi.org/10.1128/AAC.50.3.1021-1033.2006>.
48. Rathore SS, Raman T, Ramakrishnan J. 2016. Magnesium ion acts as a signal for capsule induction in *Cryptococcus neoformans*. *Front Microbiol* 7:325. <https://doi.org/10.3389/fmicb.2016.00325>.
49. Dambuzza IM, Drake T, Chapuis A, Zhou X, Correia J, Taylor-Smith L, LeGrave N, Rasmussen T, Fisher MC, Bicanic T, Harrison TS, Jaspars M, May RC, Brown GD, Yuecel R, MacCallum DM, Ballou ER. 2018. The *Cryptococcus neoformans* Titan cell is an inducible and regulated morphotype underlying pathogenesis. *PLoS Pathog* 14:e1006978. <https://doi.org/10.1371/journal.ppat.1006978>.
50. Ishida K, Rozental S, de Mello JCP, Nakamura CV. 2009. Activity of tannins from *Stryphnodendron adstringens* on *Cryptococcus neoformans*: effects on growth, capsule size and pigmentation. *Ann Clin Microbiol Antimicrob* 8:29. <https://doi.org/10.1186/1476-0711-8-29>.
51. Klepser ME, Ernst EJ, Lewis RE, Ernst ME, Pfaller MA. 1998. Influence of test conditions on antifungal time-kill curve results: proposal for standardized methods. *Antimicrob Agents Chemother* 42:1207–1212. <https://doi.org/10.1128/AAC.42.5.1207>.
52. Lee KK, Kubo K, Abdelaziz JA, Cunningham I, Dantas AS, Chen X, Okada H, Ohya Y, Gow NAR. 2018. Yeast species-specific, differential inhibition of β -1,3-glucan synthesis by poacid acid and caspofungin. *Cell Surf* 3:12–25. <https://doi.org/10.1016/j.tcs.2018.09.001>.
53. Upadhy R, Baker LG, Lam WC, Specht CA, Donlin MJ, Lodge JK. 2018. *Cryptococcus neoformans* Cda1 and its chitin deacetylase activity are required for fungal pathogenesis. *mBio* 9:e02087-18. <https://doi.org/10.1128/mBio.02087-18>.
54. Oliveira HC, Castelli RF, Reis FCG, Samby K, Nosanchuk JD, Alves LR, Rodrigues ML. 2022. Screening of the pandemic response box reveals association between antifungal effects of MMV1593537 and the cell wall of *Cryptococcus neoformans*, *Cryptococcus deuterogattii*, and *Candida auris*. *Microbiol Spectr* 10:e00601-22. <https://doi.org/10.1128/spectrum.00601-22>.
55. Loh JMS, Adenwalla N, Wiles S, Proft T. 2013. *Galleria mellonella* larvae as an infection model for group A streptococcus. *Virulence* 4:419–428. <https://doi.org/10.4161/viru.24930>.
56. Mylonakis E, Moreno R, Khoury JBE, Idnurm A, Heitman J, Calderwood SB, Ausubel FM, Diener A. 2005. *Galleria mellonella* as a model system to study *Cryptococcus neoformans* pathogenesis. *Infect Immun* 73:3842–3850. <https://doi.org/10.1128/IAI.73.7.3842-3850.2005>.